Parasites & Vectors

RESEARCH

Open Access

Assessment of the monthly risk of dirofilariosis infection in Europe and its projection to 2100 under climate change from a One Health perspective

Iván Rodríguez-Escolar[1], Alfonso Balmori-de la Puente[1*], Elena Infante González-Mohino[1], Manuel Collado-Cuadrado[1], Elena Carretón[2], José Alberto Montoya-Alonso[2] and Rodrigo Morchón[1,3*]

Abstract

Background Dirofilariosis is a vector-borne zoonotic disease primarily caused by the parasitic nematodes *Dirofilaria immitis* and *D. repens*. In Europe, the disease has expanded from traditionally endemic southern countries to central and northeastern regions, many of which are now also considered endemic. This study aimed to generate infection risk maps for dirofilariosis in Europe using ecoinformatic tools, at both annual and monthly scales, to serve as a prevention tool and contribute to more effective control of the disease, as well as helping to stop its spread.

Methods A habitat suitability map was generated for the two most important and widely distributed culicid vectors in Europe (*Culex pipiens* and *Aedes albopictus*). This map was weighted with the number of *D. immitis* generations in the vectors, both annually and monthly. The resulting annual risk map was validated with georeferenced records of *D. immitis*- and *D. repens*-infected dogs and cats. In addition, a future habitat suitability projection for both vector species was performed for the year 2100 under the Representative Concentration Pathway (RCP) 8.5 climate change scenario.

Results Dirofilariosis infection risk in Europe is highest in southern countries, where favorable climatic conditions and increased vector activity coincide. Central Europe showed medium- to high-risk values, while northern latitudes exhibited low or very low risk, correlating with lower average temperatures. Of the geolocated infected animals, 35.9%, 51% and 13% were located in high-, medium-, or low-risk areas, respectively. Infection risk appears to be very limited during winter, restricted mainly to Mediterranean coastal areas, the Canary Islands (Spain), and Madeira (Portugal); while in spring/summer it becomes high in these places and moderate across other parts of the range such us central and northeastern Europe. The 2100 projection predicts a 161.6% increase in habitat suitability for the vectors, particularly in northeastern regions, high-altitude areas, and northernmost countries.

Conclusions The combined use of habitat suitability for *Culex pipiens* and *Aedes albopictus* and the number of *Dirofilaria* spp. generations allowed the development of a more comprehensive color-coded dirofilariosis infection risk map than previously available. Monthly infection risk maps across Europe could help guide targeted prevention

*Correspondence:
Alfonso Balmori-de la Puente
a.balmori@usal.es
Rodrigo Morchón
rmorgar@usal.es
Full list of author information is available at the end of the article

and control measures, disrupt disease establishment in specific areas and seasons, and raise awareness about infection risks in both animals and humans.

Keywords Europe, Dirofilariosis, *Dirofilaria immitis*, *Dirofilaria repens*, *Culex pipiens*, *Aedes albopictus*, Ecological niche model, Number of generations of *Dirofilaria* spp., Annual infection risk, Monthly infection risk

Background

Species of the genus *Dirofilaria* are parasitic nematodes responsible for dirofilariosis, a vector-borne zoonotic disease. The two most relevant species are *Dirofilaria immitis* (heartworm disease) and *D. repens* (subcutaneous dirofilariosis). The definitive hosts of these parasites include both domestic and wild canids and felids, with domestic dogs serving as the main reservoir. Other hosts such as domestic cats, ferrets, and wild carnivores may also be affected [1, 2], while humans are considered accidental hosts [3, 4]. Culicid mosquitoes, including species of the genera *Culex*, *Aedes*, *Anopheles*, and *Coquillettidia*, act as vectors of the parasites [5, 6].

Both *D. immitis* and *D. repens* adults release microfilariae into the bloodstream of their definitive hosts. When mosquitoes take a blood meal, they ingest these microfilariae, which then undergo two molts within the vector to develop into the infective third-stage larvae (L_3). Upon subsequent blood feeding, the mosquito inoculates the L_3 larvae into a new host. This developmental process is temperature-dependent, taking approximately 16–20 days at 22 °C, and only 8–10 days at 28–30 °C. Temperatures below 14 °C inhibit larval development but preserve their viability [7].

In Europe, dirofilariosis is a dynamic disease, regarded for years as emerging or re-emerging, and is currently present across much of the continent. Heartworm disease was historically endemic only in Mediterranean countries (Spain, France, Greece, Italy, Portugal, and Turkey). However, *D. immitis* has now been reported in Albania, Germany, Austria, Bulgaria, Czech Republic, Croatia, Slovakia, Hungary, Moldova, Romania, Serbia, southern Russia, and Ukraine, many of which are now considered endemic areas [8–10]. Similarly, *D. repens*, previously confined to southern and southeastern regions (e.g., Bulgaria, Spain, Greece, Italy, Romania, and Turkey), has spread over the past decade to central and northern European countries such as Germany, Austria, Belarus, Slovakia, Estonia, Hungary, Latvia, Lithuania, Poland, and Ukraine [1, 5, 9–14].

The distribution and expansion of dirofilariosis is influenced by numerous environmental and social factors, including climate change, the introduction of new vector species, increased anthropogenic activity (e.g., irrigation zones, urban development, and the creation of stagnant water bodies), enhanced transportation networks, and the greater movement of people and animals. This includes a growing number of pets traveling to endemic or imported case-reporting areas [1, 8]. Some health-based control measures include preventive treatment in domestic animals, avoidance of mosquito bites, and the diagnosis and treatment of all hosts involved [4, 15]. In addition, predictive mapping tools based on ecological niche modeling (ENM) have been developed. These models estimate infection risk by correlating vector and host presence records with environmental variables [16, 17]. ENMs have been used to model the distribution of infected hosts [18–22] and vectors involved in transmission [23, 24, 89, 90, 91, 92, 93, 94, 95], as well as to assess infection risk by integrating the potential distribution of one or more vectors and the parasite's development within them [25–27].

Several local and national studies in Europe have estimated the risk of dirofilariosis transmission solely on the basis of temperature records [28–37]. More recently, models have integrated habitat suitability and the estimated number of annual *Dirofilaria* spp. generations in vectors in countries such as Spain, Greece, Italy, Portugal, and Serbia [25, 38–41]. At the continental level, infection risk has so far only been estimated by calculating the number of annual generations of *Dirofilaria* spp. within vectors [42, 43].

Therefore, the aim of this study was to assess the risk of dirofilariosis infection across Europe by generating colorimetric maps at both monthly and annual scales. These maps are based on ecological niche modeling of the main vectors and the estimated number of parasite generations within them. In addition, the study projects vector habitat suitability by the year 2100 under climate change scenarios. This approach seeks to provide a useful prevention and control tool for medical and veterinary professionals, pet owners, and the general public, within a One Health framework.

Methods

Study area: Europe

Europe covers about 10 million km^2 in the Northern Hemisphere, bordered by the Arctic Ocean to the north, the Atlantic Ocean to the west, and the Mediterranean Sea to the south [44]. The most widespread climate according to the Köppen–Geiger classification is humid continental (Df), located in the center and east of the

continent, with cold winters, cool summers, and rainfall throughout the year. Countries near the Mediterranean Sea have a Mediterranean climate (typical Mediterranean climate [Csa] and typical Mediterranean climate with warm summers [Csb]), with mild winters, dry and warm summers, and rainfall concentrated mainly in spring and autumn. Western Europe has an oceanic climate (Cfb) with cold or mild winters, cool summers, and rainfall throughout the year. In northern Europe, the predominant climate is subarctic continental (Dfc), characterized by very cold, long winters with snowfall and cold summers. Finally, in the far north, there are areas with a tundra climate (ET), where the average temperature does not exceed 10 °C in any month. Noteworthy are the Canary Islands (Spain), as well as the Azores and Madeira (Portugal), which have subtropical characteristics, with mild temperatures throughout the year, dry summers, and significant variations in rainfall [45, 46].

Presence data

Geolocated presence points for the dirofilariosis vectors *Cx. pipiens* (8691) and *Ae. albopictus* (19,878) were obtained from: (1) the Global Biodiversity Information Facility (GBIF) data repository [47]; (2) the European Network for Medical and Veterinary Entomology of the European Centre for Disease Prevention and Control [48]; and (3) additional reported data [38, 49–56]. These vectors are the most important and widely distributed culicid mosquito species on the European continent [8, 57]. These data were processed to avoid spatial autocorrelation biases in the abundance and distribution of observations. A 1 km^2 grid was superimposed, leaving only one observation per square. At the end of the process, the number of presence points was 2502 for *Cx. pipiens* and 2378 for *Ae. albopictus* (Supplementary Fig. S1).

Bioclimatic and environmental variables

In total, 19 bioclimatic variables (1970–2000) related to temperature and precipitation were downloaded from the WorldClim climate database [58], both for the present and for projections to 2100 under a climate change scenario. To avoid cross-correlation and improve model calibration, a multicollinearity test was performed in R software [59] using Pearson's correlation coefficient. Variables with a correlation coefficient equal to or greater than 0.8 were discarded [60]. After this analysis, the selected variables were: annual mean temperature (BIO_1), isothermality (BIO_3), temperature seasonality (BIO_4), mean temperature of wettest quarter (BIO_8), mean temperature of driest quarter (BIO_9), annual precipitation (BIO_{12}), and precipitation seasonality (BIO_{15}). In addition, a series of environmental variables important for vector survival were also downloaded: human footprint (built environment, population density, electrical energy infrastructure, cropland, grazing land, roads, railways, and waterways) [61], rivers, water bodies, irrigated crops [62], and shrub and herbaceous density [63]. All downloaded variables had a resolution of 1 km^2 per pixel and were processed in ArcMap 10.8 software to crop them to the same extent (the European continent) and give them the same coordinates (GCS_WGS_1984).

Ecological niche models

To generate habitat suitability models for *Cx. pipiens* and *Ae. albopictus*, the MaxEnt algorithm [64] was used, automated by the Kuenm package [60] in R software [59]. MaxEnt calculates the habitat suitability of species on the basis of their climatic and environmental requirements, and Kuenm generates all possible models with parameter combinations and selects the best one, taking into account statistical significance (partial receiver operating characteristic [ROC] < 0.05) with 100 iterations and 50% of the presence data used for bootstrapping, the omission rate (OR = 5%), and complexity using the Akaike information criterion. A total of 119 models were generated for each species by combining the following parameters: a single set of variables, 17 regularization multiplier values "M" (0.1–1.0 at intervals of 0.1; 2–6 at intervals of 1, 8, and 10), and seven possible combinations of three feature classes "F" (linear, quadratic, and product). All generated models were validated with the mean ratio of the area under the curve (AUC), using independent occurrence points (80% for training and 20% for testing). The final habitat suitability models for *Cx. pipiens* and *Ae. albopictus*, selected on the basis of the best performance according to Kuenm's criteria, were generated again using the clamping extrapolation option, obtaining ten replicates with the same combination of parameters chosen in the previous step. The pixels composing the habitat suitability maps for both species of culicid mosquitoes were weighted in the same proportion (50–50) using the following formula, where ENMc and ENMa are the habitat suitability values for *Cx. pipiens* and *Ae. albopictus* models, respectively:

$$\text{ENM weighted} = \frac{\text{ENMc}*50 + \text{ENMa}*50}{100}$$

Dirofilaria spp. generations

We calculated the number of generations of *Dirofilaria* spp. per year and in each of the 12 months of the year using the method described by Rodríguez-Escolar et al. [25] and Genchi et al. [42] based on our own R script. This methodology adds up the degrees Celsius (growing degree days or GDDs) in which the average daily temperature exceeds 14 °C, the minimum threshold

necessary for the development of L_3 larvae of the parasite in the mosquito (extrinsic incubation). A complete generation requires at least 130 GDDs within the mosquito's lifespan, within a maximum of 30 days. The number of generations of *Dirofilaria* spp. per year were calculated by averaging the generations contained in each of the 12 months. To perform these calculations, the most up-to-date variables of average daily temperature across the continent from 1990 to 2016 were downloaded [65].

Dirofilaria spp. risk map and its validation

The habitat suitability model for both species was weighted by the number of generations of *Dirofilaria* spp. in a year and in each of the 12 months in the same proportion (50–50), obtaining an average infection risk map for the whole of Europe and, in addition, a risk map for each month of the year, using the following formula:

$$Riskmap = \frac{ENMweighted * 50 + GenerationsofDirofilaria * 50}{100}$$

To validate the average infection risk map, we used the Natural Jenks classification method (breaks) in ArcMap with five risk classes ("very high," "high," "medium," "low," and "very low"). The georeferenced points of dogs and cats infected with *D. immitis* or *D. repens* (5408) were obtained from myVBDmap [66] and other scientific reports [8, 41, 57, 67–74] and superimposed on the average risk map.

Projection to the year 2100 and rank-change analysis

To make the projection for the year 2100, the ENMs for both vectors were generated again using the same parameters selected for the models generated today but incorporating the projections of the bioclimatic variables for the period 2081–2100. The HadGEM3-GC31-LL model was used to analyze the effect of climate change under the Representative Concentration Pathway (RCP) 8.5 scenario [75, 76], one of the most widely used and evaluated general circulation models (GCM) in ecological niche modeling studies, as it adequately captures important climate patterns for Europe [77, 78]. The current model (present) and the model for the year 2100 (future) were transformed into binary maps of presence and absence using the 10th percentile threshold of the current map. Finally, a range change analysis was performed using the R package biomod2, which calculates the percentage of pixels that gain or lose habitat suitability for both vectors in the year 2100 compared with the current model [79].

Results

Habitat suitability models for *Cx. pipiens* and *Ae. albopictus*

Out of the 119 habitat suitability models generated for each vector, the model M_0.3_F_lqp (AUC = 0.828) was selected for *Cx. pipiens*, and M_0.1_F_lp (AUC = 0.877) for *Ae. albopictus*, as they best met the Kuenm selection criteria (Supplementary Fig. S2). Regarding variable contribution, for the *Cx. pipiens* habitat suitability model, the most influential variables were BIO_4 (temperature seasonality), water bodies, and human footprint, contributing 22.7%, 22.7%, and 20.9%, respectively. In the case of the *Ae. albopictus* model, the top contributing variables were human footprint (20%), BIO_1 (mean annual temperature, 16.6%), and water bodies (13.3%). The least influential variables in both models were river proximity and shrubland density (Table 1). Using an equal weighting scheme (50–50), the two models were combined to generate a final habitat suitability map for both vectors. The most suitable habitats were located in areas with higher average temperatures, coastal regions, river-adjacent zones, urban environments, and irrigated agricultural lands. High suitability was observed across southern countries (Spain, Portugal, France, Italy, and Greece), as well as along the Adriatic and Black Sea coasts, southwestern UK, the Belgian and Dutch coastlines, and areas near major rivers in central Europe (Fig. 1).

Number of extrinsic generations of *Dirofilaria* spp.

Supplementary Fig. S3 shows the average annual number of *Dirofilaria* spp. extrinsic generations in vectors across Europe. The highest number of generations (> 4) occurred mainly in southern European regions, such as the southwestern Iberian Peninsula and the archipelagos of the Canary Islands, Azores, and Madeira (Spain

Table 1 Percentage contribution of the variables selected in the ecological niche model for *Cx. pipiens* and *Ae. albopictus*

Variable	Percentage contribution	
	Culex pipiens (%)	*Aedes albopictus (%)*
Water bodies	22.7	13.3
Temperature seasonality (BIO_4)	22.7	13.1
Human footprint	20.9	20
Annual mean temperature (BIO_1)	16	16.6
Isothermality (BIO_3)	6.5	11.4
Mean temperature of driest quarter (BIO_9)	4.2	9.8
Precipitation seasonality (BIO_{15})	2.7	4
Annual precipitation (BIO_{12})	1.7	2.7
Mean temperature of wettest quarter (BIO_8)	0.7	6.3
Herbaceous density	0.7	1
Shrub density	0.5	0.23
Irrigated crops	0.5	1.4
Rivers	0.1	0.2

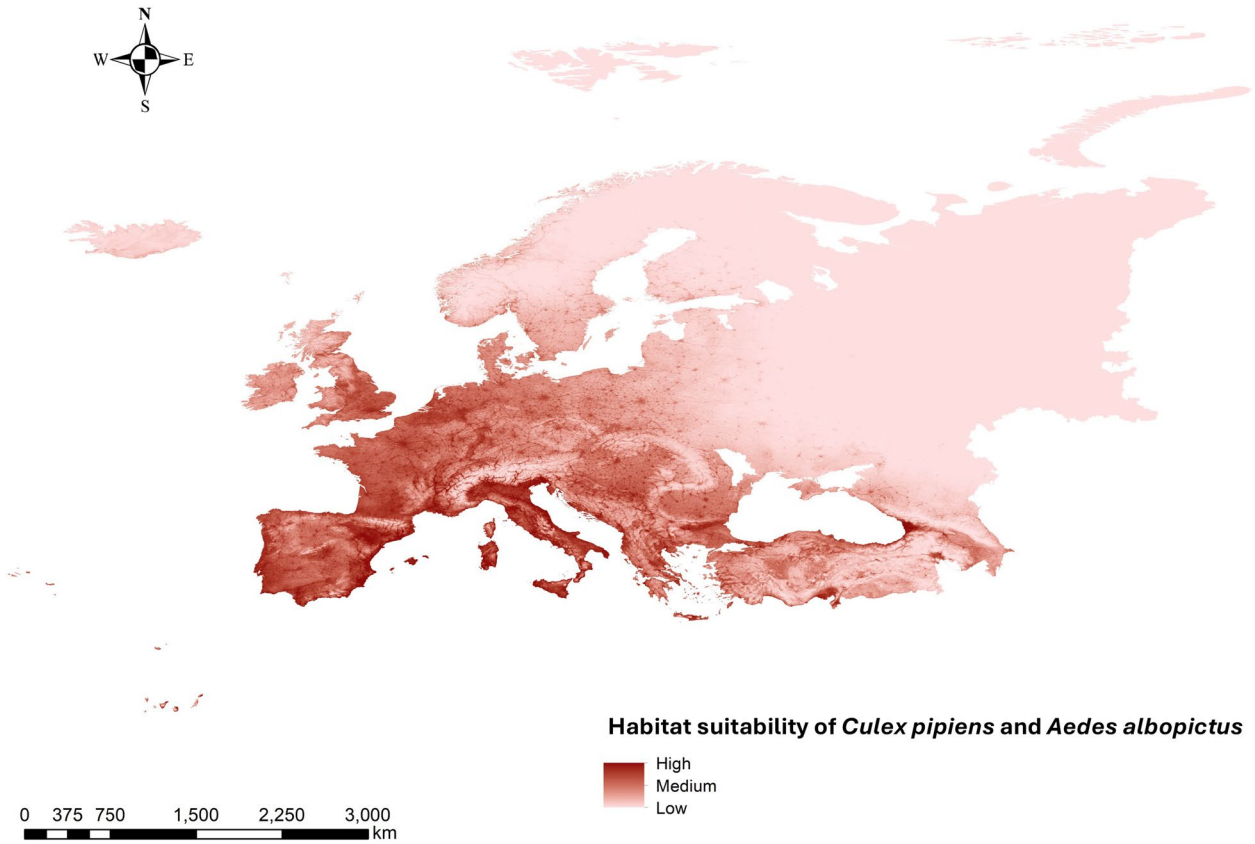

Fig. 1 Weighted (50–50) habitat suitability map (ecological niche model) for *Culex pipiens* and *Aedes albopictus* in Europe

and Portugal), as well as along Mediterranean coastal areas—including the Levantine coast and Balearic Islands (Spain), Sicily and Sardinia (Italy), the Aegean coastline and islands (Greece), and the southeastern coast of Anatolia (Turkey). The lowest number of generations was found in mountainous areas and in northern Europe.

Regarding the monthly generation maps (Fig. 2), July showed the greatest number of locations with a high number of generations, with very high values (>8) across Mediterranean countries (Spain, Portugal, southern France, Italy, Greece, and Turkey), and moderate-to-high values across most of the continent, except in northern latitudes and high-altitude mountain areas. In contrast, January had the lowest generation numbers, reaching zero across nearly all of Europe, except for some coastal Mediterranean zones.

Annual infection risk map for dirofilariosis and its validation

The resulting map from the weighted combination of both vector ENMs and the average generation map for *Dirofilaria* spp. is shown in Fig. 3a. This map represents the average annual risk of dirofilariosis infection across Europe. The highest infection risk areas were mainly located in southern countries, such as Spain and Portugal—particularly in the southwestern Iberian Peninsula, the Levantine coast, the Ebro Basin, the Balearic and Canary Islands (Spain), and the Azores (Portugal). Other high-risk regions included the French Riviera, the Italian coastline (including Sicily and Islands of Sardinia) with the Po Valley, Albania, the Aegean region, and southwestern Turkey. Central Europe presented medium-to-high infection risk values, whereas northern latitudes (e.g., the Scandinavian Peninsula, northern UK), characterized by lower temperatures, displayed low or very low infection risk. The validation of the model (Fig. 3b), using 5408 georeferenced infection cases, showed that 35.9% occurred in high/very high-risk zones, 51% in medium-risk zones, and 13% in low-risk zones.

Monthly infection risk maps for dirofilariosis

Analysis of monthly risk maps throughout the year (Fig. 4) revealed that during the winter months, infection risk was very low across almost the entire continent, except for some coastal areas of Mediterranean countries (Spain, Portugal, Italy, Greece, and France).

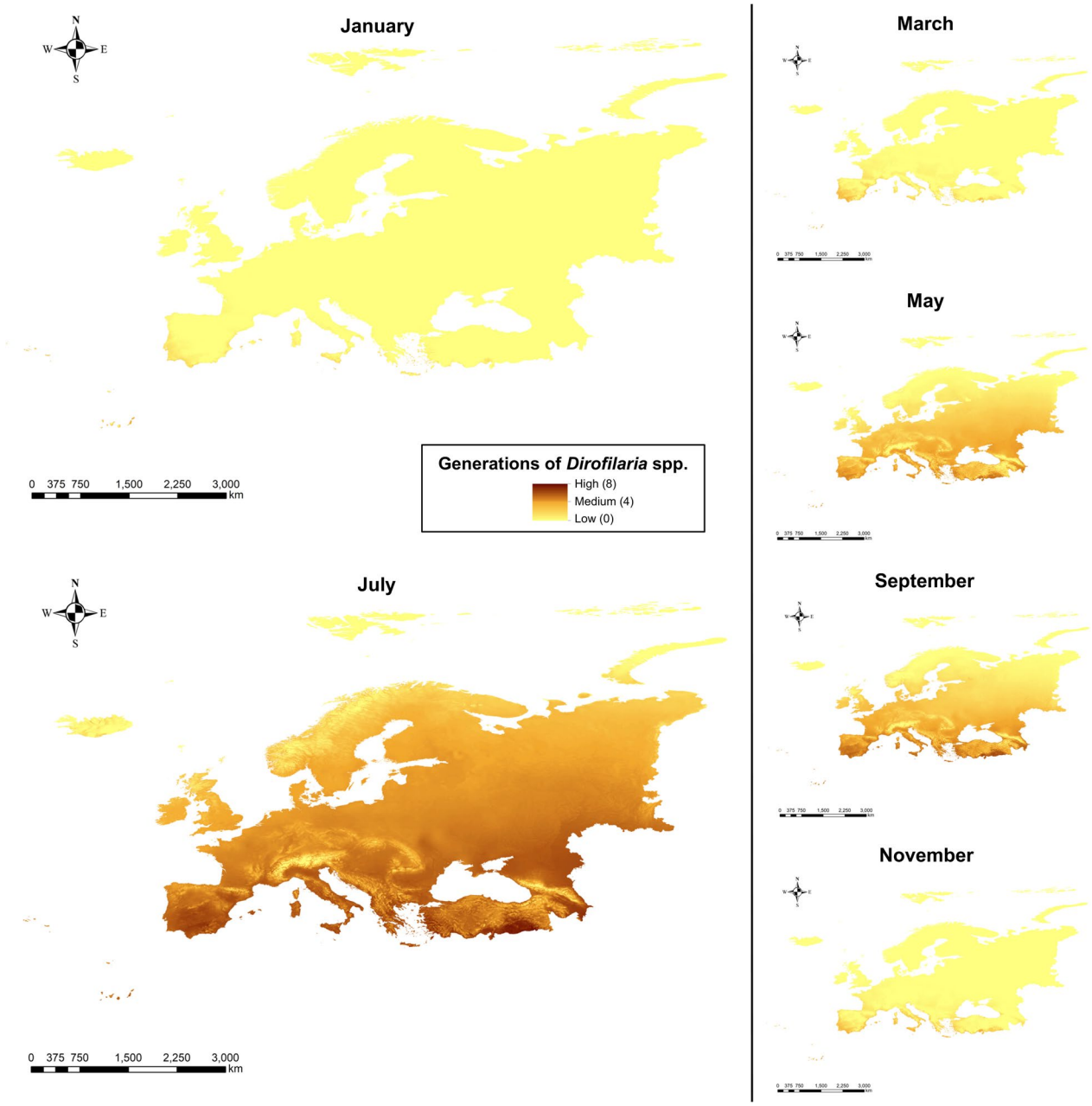

Fig. 2 Number of generations of *Dirofilaria* spp. in Europe every 2 months (January, March, May, July, September, and November)

In spring, infection risk gradually increased from south to north. In summer (Fig. 5), infection risk rose significantly across most of the continent, except at higher latitudes (northern UK, northern Russia, and Scandinavia) and in mountainous areas. Southern Europe, with its warmer climate, showed very high infection risk values, while central Europe ranged from moderate to high risk. Finally, during autumn, infection risk declined gradually from north to south.

Projection of habitat suitability for vectors in 2100

The future projection of habitat suitability for *Cx. pipiens* on 2100, under a climate change scenario, generated a gain of 84.89% and a loss of 0.11%. For *Ae. albopictus*, the gain in habitat suitability was 336.13% and the

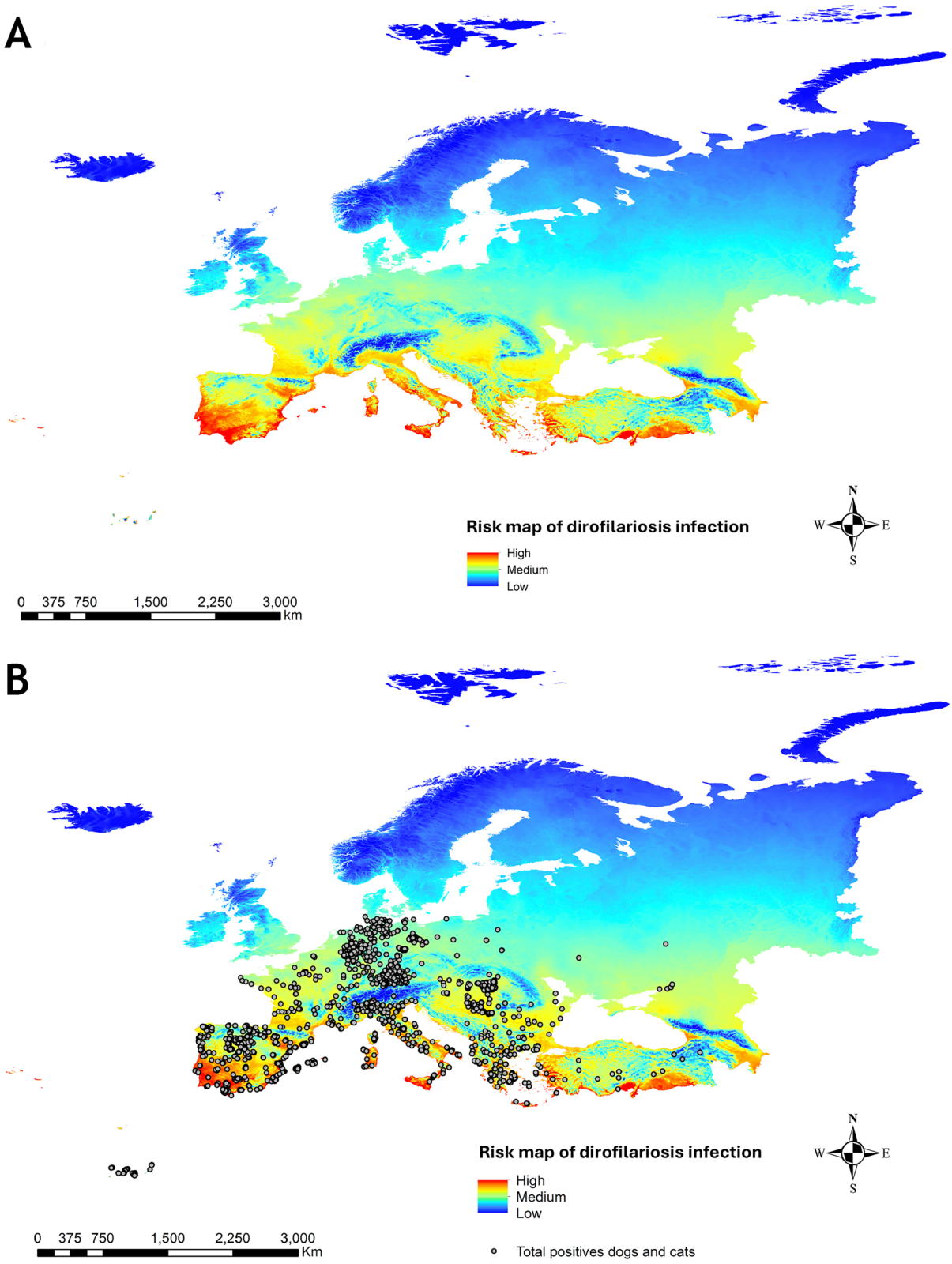

Fig. 3 **A** Risk map of dirofilariosis infection in Europe and **B** with the georeferenced points of dogs and cats infected with *D. immitis* or *D. repens*

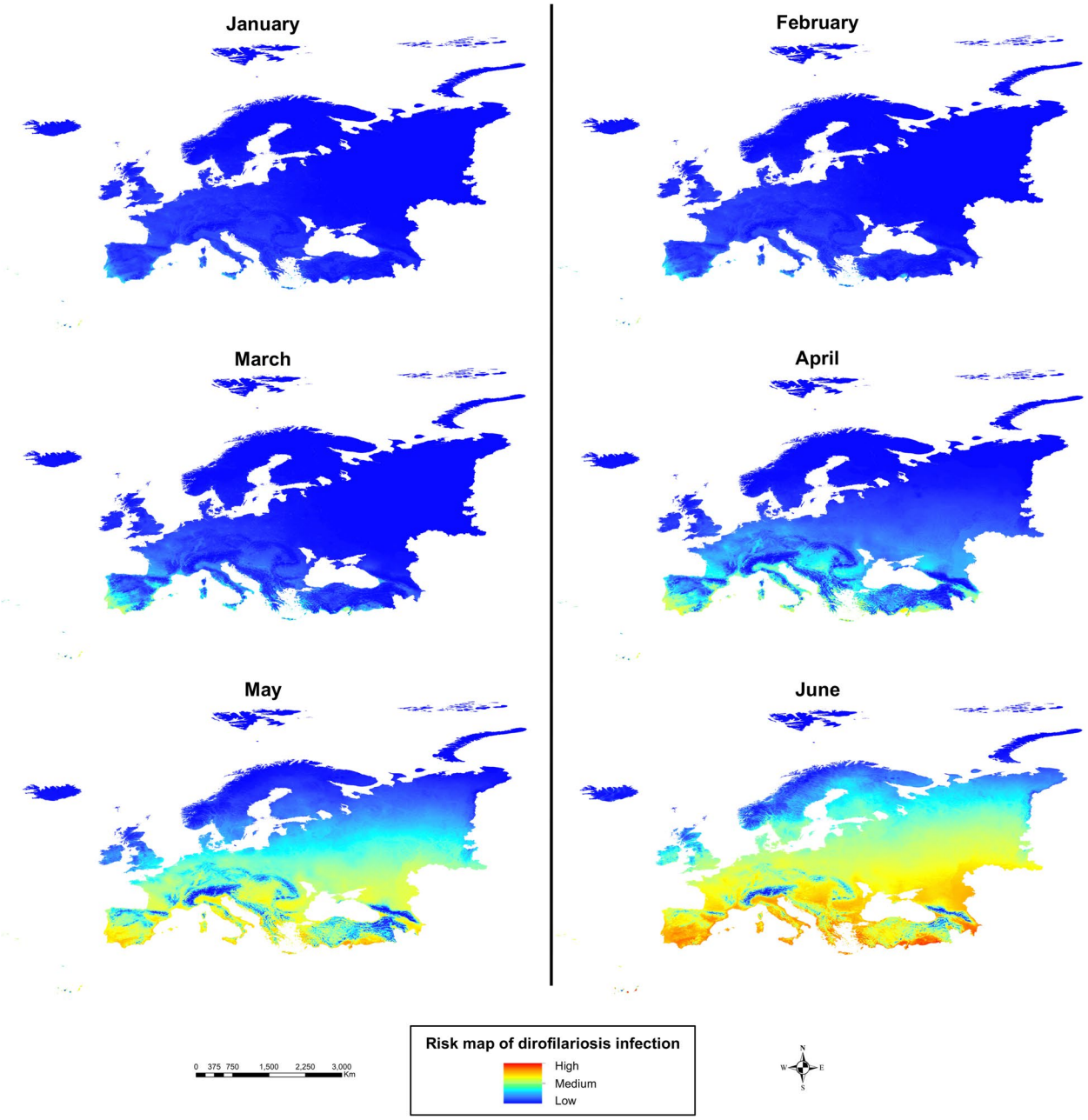

Fig. 4 Risk map of dirofilariosis infection in Europe from January to June (first 6 months of the year)

loss was 1.06% (Supplementary Fig. S4). The future projection for both species (Fig. 6a) shows a considerable increase in habitat suitability for both vectors. The range-change analysis for each species is shown in Supplementary Fig. S5 and for both species in Fig. 6b. The latter indicates a 161.6% increase in suitability at the European territory level. This increase occurs mainly in the north-eastern regions of the continent, at higher latitudes, and in higher altitude areas, which currently have cold climates and low suitability for the presence of these vectors. In the rest of the territories, the risk remains stable.

Discussion

In Europe, dirofilariosis has continued to expand over recent decades [3–5, 8]. Several factors are associated with this expansion, including climate change, the

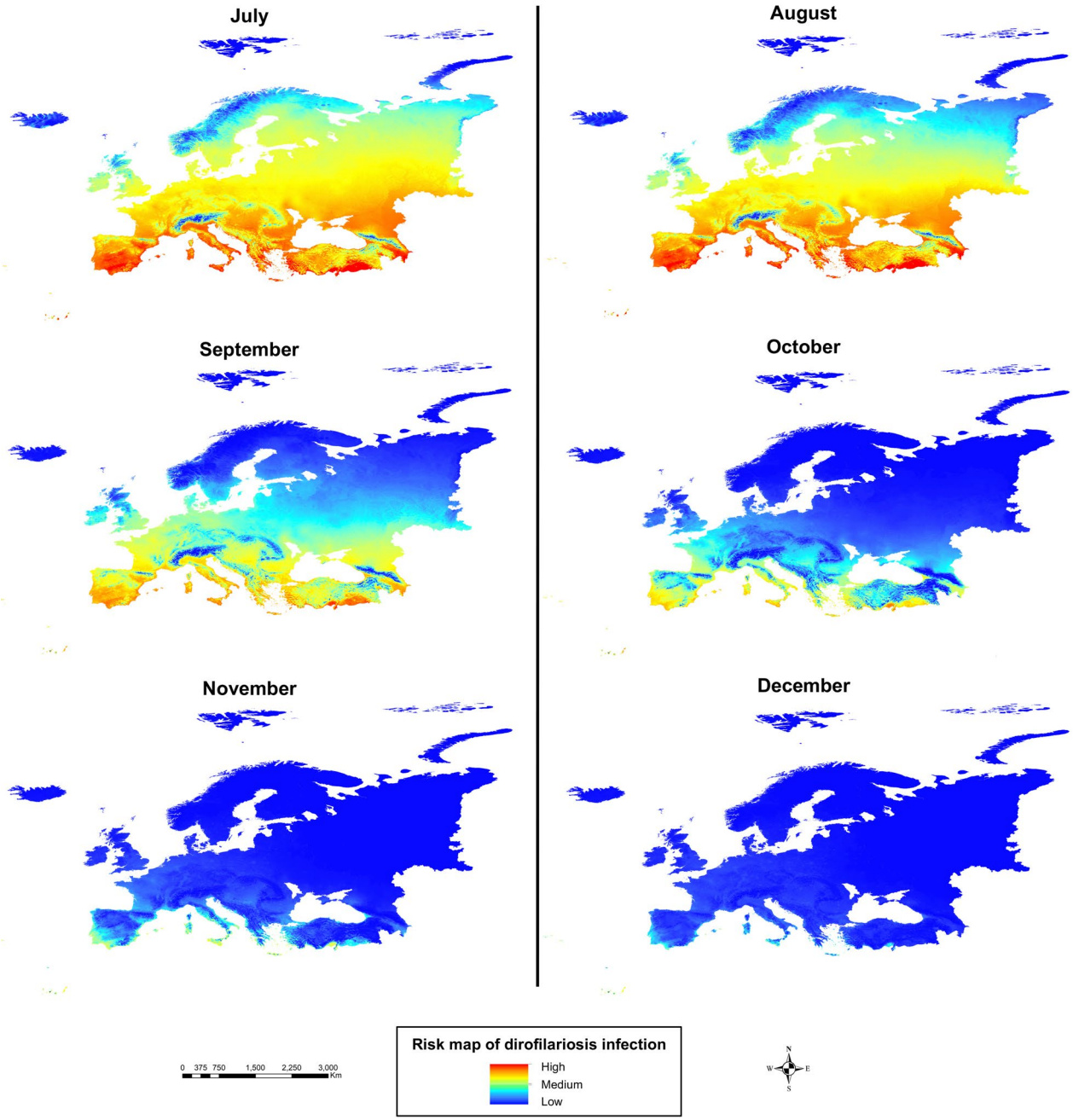

Fig. 5 Risk map of dirofilariosis infection in Europe from July to December (last 6 months of the year)

increasing number of pet travel, and the lack of preventive actions in animal hosts [8, 15].

Studies aiming to assess the infection risk of dirofilariosis in Europe as a control strategy are still scarce. Some have relied exclusively on temperature records, often assuming an oceanic climate throughout Western Europe with sufficient humidity and warmth for the parasite to develop within the vector [30, 35, 36, 38, 42, 43, 80]. Other studies, conducted at national or regional scales in Spain, Portugal, Italy, Serbia, and Greece, have integrated habitat suitability models for one vector species with the estimated development of *Dirofilaria* spp. within that vector [25, 39–41]. However, these efforts remain geographically limited and fail to provide an integrated overview of the infection risk across the entire European continent.

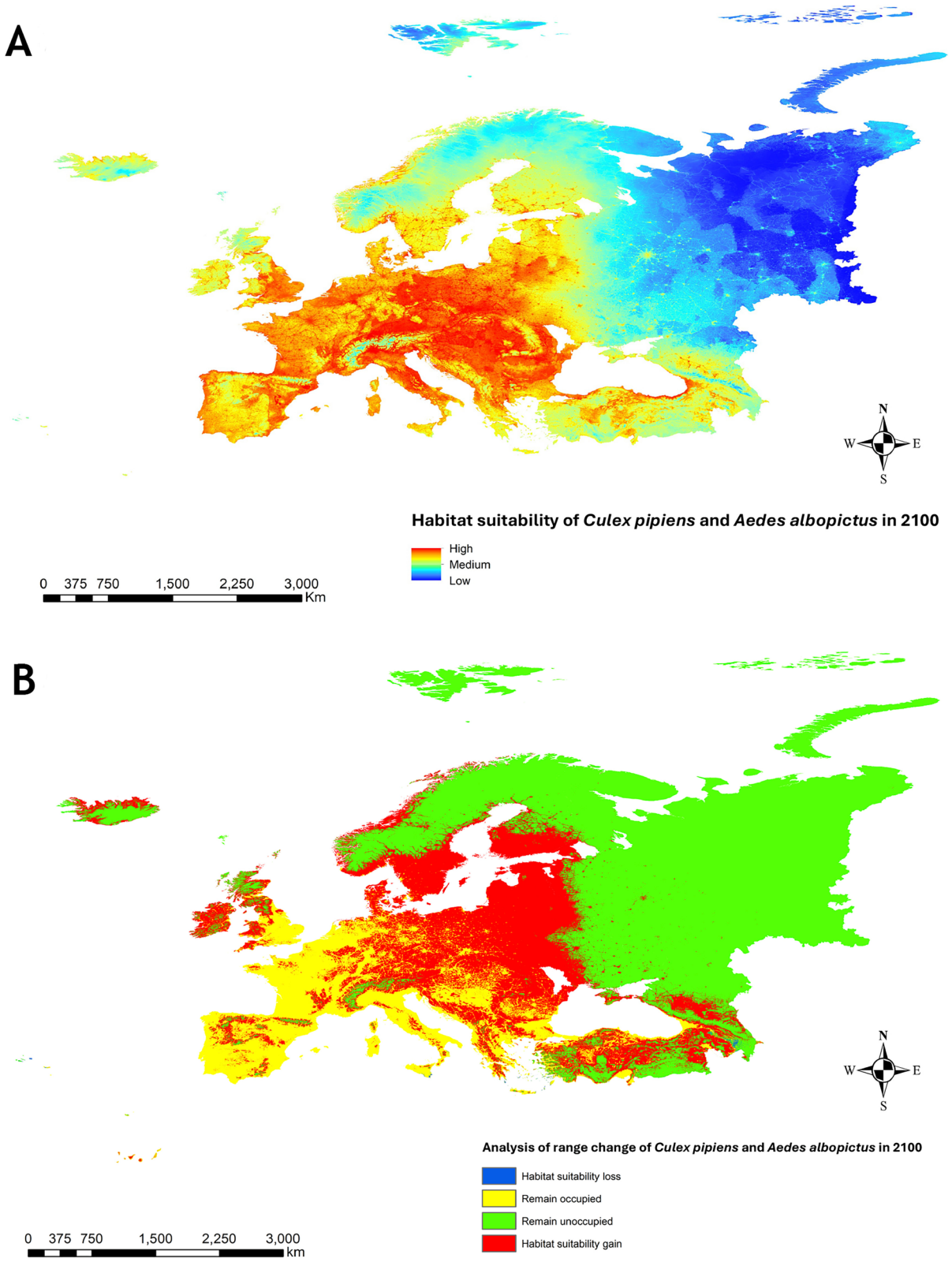

Fig. 6 **A** Projection of weighted (50–50) habitat suitability for *Cx. pipiens* and *Ae. albopictus* in Europe for the year 2100 under the RCP 8.5 climate change scenario. **B** Range-change analysis of weighted (50–50) range change for *Cx. pipiens* and *Ae. albopictus* in Europe for the year 2100, showing areas of gain and loss and those that remain unchanged in terms of habitat suitability

In our study, we evaluated the potential risk of *Dirofilaria* spp. infection across Europe by generating a color-coded map at both annual and monthly scales. This was carried out by modeling the habitat suitability of the two most relevant and widely distributed vector species in Europe (*Culex pipiens* and *Aedes albopictus*) using ecological niche models (ENMs), and weighting these maps by the estimated number of parasite generations within the vector. This approach represents a significant advancement, as it yields temporally targeted depiction of the current infection risk across Europe. In addition, the high spatial resolution (~1 km^2) allows for the development of more localized prevention strategies.

The ENMs developed for both vector species yielded high AUC values (>0.8), indicating strong predictive performance in discriminating between presence locations and background environmental conditions. The most influential variables in the distribution of *Cx. pipiens* were temperature seasonality (BIO_4) and proximity to water bodies (22.7% each), while for *Ae. albopictus*, human footprint and mean annual temperature (BIO_1) were the main contributors (≥16.6% each). This confirms the pivotal role of temperature-related variables in vector survival, with low precipitation acting as a limiting factor for mosquito establishment [8, 81, 82]. However, the negative effects of low rainfall are often compensated by the presence of natural and artificial water bodies, irrigated agricultural zones, and urban areas that provide suitable habitats for vector reproduction—areas where previous studies have reported high prevalence of canine dirofilariosis [74]. In the case of *Ae. albopictus*, the high contribution of human footprint as a predictor variable aligns with its well-known anthropophilic and urban-adapted behavior [41, 83]. Therefore, it is not surprising that aside from temperature-related factors, water availability and human activity are among the main contributors to the habitat suitability of *Cx. pipiens* and *Ae. albopictus*, respectively.

With regard to the continental risk map for dirofilariosis, high-risk zones were mainly located in areas with elevated temperatures, both natural and artificial water sources, and high human footprint—settings where dogs and humans coexist closely, increasing the zoonotic infection potential [1, 8]. Conversely, colder regions and mountainous zones presented low risk values, in line with the limited vector presence reported in such areas. Monthly infection risk maps revealed seasonal variation, with very low risk during winter months except for some coastal Mediterranean areas. Risk increased progressively throughout spring, reaching its peak in summer across most of Europe—except in the highest latitudes and mountainous areas—consistent with the seasonal dynamics of the disease described in previous studies [28, 42, 43].

Our projection for the year 2100 suggests a 161.6% increase in habitat suitability for both vector species as a result of climate change. This projection indicates a potential spread of *Cx. pipiens* and *Ae. albopictus* into northeastern Europe, more northern latitudes, and mountainous regions—areas that were previously non-endemic—unless control measures are implemented. Climate change appears to influence the thermal limits for transmission, which may substantially alter the seasonal patterns and geographic distribution of zoonotic diseases in cooler countries, as reflected in our findings [35, 84–88].

An additional factor that may influence the distribution and persistence of dirofilariosis, particularly in southern Europe, is the growing population of stray or unowned dogs and cats. These animals often remain outside veterinary surveillance programs and do not receive prophylactic treatment, enabling the maintenance of local transmission cycles even in areas where preventive measures are widely applied to owned pets. Their presence in urban and periurban environments, frequently overlapping with high-risk zones identified on our maps, may thus contribute to sustaining parasite circulation and reintroduction after control efforts. Incorporating data on stray animal populations and their infection rates into future models would improve the accuracy of risk assessment and help design more effective One Health-based intervention strategies.

Among the limitations of our study, the vector component should be highlighted first. The present records compiled from GBIF/VectorNet and literature are subject to spatial sampling biases and temporal heterogeneity. Furthermore, the 50–50 weighting of the two vector ENMs implicitly assumes an equal contribution across space and seasons, whereas vector competition, urban versus rural bionomics, and diapause vary geographically. Second, the thermal development module uses generalized thresholds (≥14 °C; ≥130 GDD in ≤30 days) and does not explicitly account for humidity, vector longevity, microclimatic effects (e.g., urban heat islands), or nonlinear thermal responses. Third, environmental layers and different time bases may smooth microhabitats and introduce temporal mismatch. Fourth, validation using georeferenced cases of dogs and cats is limited by underreporting, diagnostic variability, uncertainty about the timing of infection, travel history, and geolocation inaccuracies; consequently, monthly risk could not be empirically validated. Finally, climate projections were based on a single global climate model and a high emissions pathway, which does not reflect structural and scenario uncertainty. These caveats delineate priorities for future work, including multivector ENMs with biased background correction,

integration of host and intervention layers, joint climate projections, and prospective entomological and serological validation with monthly resolution.

Conclusions

This study presents the first Europe-wide assessment of *Dirofilaria* spp. infection risk. The spatiotemporal maps show a clear seasonal pattern, with risk increasing from winter to summer and peaking in July, particularly in southern and Mediterranean regions where conditions favor vector and parasite development. These maps provide a valuable tool for guiding surveillance, diagnosis, and control of dirofilariosis in Europe. Their application supports targeted prevention, prioritization of intervention areas, and incorporation of the One Health approach into the management of this emerging vector-borne zoonosis.

Abbreviations

Ae. Albopictus	*Aedes albopictus*
AUC	Area under the curve
BIO_1	Annual mean temperature
BIO_3	Isothermality
BIO_4	Temperature seasonality
BIO_8	Mean temperature of wettest quarter
BIO_9	Mean temperature of driest quarter
BIO_{12}	Annual precipitation
BIO_{15}	Precipitation seasonality
Cfb	Oceanic climate
Csa	Typical Mediterranean climate
Csb	Typical Mediterranean climate with warm summers
Cx. pipiens	*Culex pipiens*
D. immitis	*Dirofilaria immitis*
D. repens	*Dirofilaria repens*
Df	Humid continental climate
Dfc	Subarctic continental climate
ENM	Ecological niche model
ENMa	Habitat suitability model for *Ae. albopictus*
ENMc	Habitat suitability model for *Cx. pipiens*
ET	Tundra climate
GDDs	Growing degree days

Supplementary Information

The online version contains supplementary material available at https://doi.org/10.1186/s13071-025-07148-5.

Additional file 1 (Supplementary Figure 1. Geolocated points of Cx. pipiens and Ae. albopictus in Europe.)

Additional file 2 (Supplementary Figure 2. Habitat suitability map (Ecological niche model) for Culex pipiens (A) and Aedes albopictus (B) in Europe.)

Additional file 3 (Supplementary Figure 3. Number of extrinsic generations of Dirofilaria spp. in Europe.)

Additional file 4 (Supplementary Figure 4. Projection of habitat suitability of Cx. pipiens (A) and Ae. albopictus (B) in Europe for the year 2100 under the RCP 8.5 climate change scenario.)

Additional file 5 (Supplementary Figure 5. Range change Analysis of range change of Cx. pipiens (A) and Ae. albopictus (B) in Europe for the year 2100 showing areas of gain, loss and those that remain unchanged in terms of habitat suitability.)

Acknowledgements
Not applicable.

Author contributions
RM designed and coordinated the study. IR-E, EIG-M, AB-dlP, MC-C, EC, and JAM-A obtained the data. IR-E and AB-dlP carried out the experimental phase and performed the analyses. IR-E, AB-dlP, and RM participated in the discussion of the results. IR-E and RM prepared the figures. IR-E, AB-dlP, and RM drafted the manuscript. All authors read, reviewed, and approved the final manuscript.

Funding
This study was supported by CEVA Santé Animale S.A. and General Fundation of University of Salamanca (art. 60 LOSU).

Availability of data and materials
Data supporting the main conclusions of this study are included in the manuscript.

Declarations

Ethical approval and consent to participate
Not applicable.

Consent for publication
Not applicable.

Competing interests
The authors declare no competing interests.

Author details
[1]Zoonotic Diseases and One Health Group, Faculty of Pharmacy, Centre for Environmental Studies and Rural Dynamization (CEADIR), University of Salamanca, Salamanca, Spain. [2]Internal Medicine, Faculty of Veterinary Medicine, Research Institute of Biomedical and Health Sciences (IUIBS), University of Las Palmas de Gran Canaria, Las Palmas de Gran Canaria, Spain. [3]Biomedical Research Institute of Salamanca (IBSAL), University of Salamanca, Salamanca, Spain.

Received: 9 August 2025 Accepted: 4 November 2025
Published online: 27 November 2025

References

1. Genchi C, Kramer LH. The prevalence of *Dirofilaria immitis* and *D. repens* in the Old World. Vet Parasitol. 2020;280:108995. https://doi.org/10.1016/j.vetpar.2019.108995.
2. Noack S, Harrington J, Carithers DS, Kaminsky R, Selzer PM. Heartworm disease-overview, intervention, and industry perspective. Int J Parasitol Drugs Drug Resist. 2021;16:65–89. https://doi.org/10.1016/j.ijpddr.2021.03.004.
3. Simón F, Diosdado A, Siles-Lucas M, Kartashev V, González-Miguel J. Human dirofilariosis in the 21st century: a scoping review of clinical cases reported in the literature. Transbound Emerg Dis. 2022;69:2424–39. https://doi.org/10.1111/tbed.14210.
4. Perles L, Dantas-Torres F, Krücken J, Morchón R, Walochnik J, Otranto D. Zoonotic dirofilariases: one, no one, or more than one parasite. Trends Parasitol. 2024;40:257–70. https://doi.org/10.1016/j.pt.2023.12.007.
5. Capelli G, Genchi C, Baneth G, Bourdeau P, Brianti E, Cardoso L, et al. Recent advances on *Dirofilaria repens* in dogs and humans in Europe. Parasit Vectors. 2018;11:663. https://doi.org/10.1186/s13071-018-3205-x.
6. Hattendorf C, Lühken R. Vectors, host range, and spatial distribution of *Dirofilaria immitis* and *D. repens* in Europe: a systematic review. Infect Dis Poverty. 2025;14:58. https://doi.org/10.1186/s40249-025-01328-2.
7. Cancrini G, Kramer L. Insect vectors of *Dirofilaria* spp. In: Simón F, Genchi C, editors. Heartworm infection in humans and animals. Salamanca: Ediciones Universidad de Salamanca; 2021. p. 63–82.

8. Morchón R, Montoya-Alonso JA, Rodríguez-Escolar I, Carretón E. What has happened to heartworm disease in Europe in the last 10 years? Pathogens. 2022;11:1042. https://doi.org/10.3390/pathogens11091042.
9. Paliy AP, Sumakova NV, Pavlichenko OV, Reshetylo OI, Kovalenko LM, Grebenik NP, Bula LV. Monitoring of animal dirofilariosis incidence in Kharkiv region of Ukraine. Zoodiversity. 2022. https://doi.org/10.15407/zoo2022.02.153.
10. Jerzsele Á, Kovács D, Fábián P, Fehérvári P, Paszerbovics B, Bali K, et al. New insights into the prevalence of *Dirofilaria immitis* in Hungary. Animals (Basel). 2025;15:1198. https://doi.org/10.3390/ani15091198.
11. Demiaszkiewicz AW, Polańczyk G, Osińska B, Pyziel AM, Kuligowska I, Lachowicz J, et al. Prevalence and distribution of *Dirofilaria repens* Railliet et Henry, 1911 in dogs in Poland. Pol J Vet Sci. 2014;17:515–7.
12. Alsarraf M, Levytska V, Mierzejewska EJ, Poliukhovych V, Rodo A, Alsarraf M, et al. Emerging risk of *Dirofilaria* spp. infection in Northeastern Europe: high prevalence of *Dirofilaria repens* in sled dog kennels from the Baltic countries. Sci Rep. 2021;11:1068. https://doi.org/10.1038/s41598-020-80208-1.
13. Deksne G, Jokelainen P, Oborina V, Lassen B, Akota I, Kutanovaite O, et al. The zoonotic parasite *Dirofilaria repens* emerged in the Baltic countries Estonia, Latvia, and Lithuania in 2008–2012 and became established and endemic in a decade. Vector Borne Zoonotic Dis. 2021;21:1–5. https://doi.org/10.1089/vbz.2020.2651.
14. Ferrara M, Maglione R, Ciccarelli D, Mundis SJ, Di Loria A, Pisaroglo de Carvalho M, Santoro D. Prevalence of *Dirofilaria* repens in dogs living in deltaic coastal plain of the Volturno River (Italy): a geographical risk model of infection. Journal of Helminthol. 2022;96:e12. https://doi.org/10.1017/S0022149X22000062.
15. Esteves-Guimarães J, Montoya-Alonso JA, Matos JI, Ramalheira E, Carretón E, Rodríguez-Escolar I, Balmori-de la Puente A, Collado-Cuadrado M, Morchón R, Fontes-Sousa AP. Raising Awareness of Canine, Feline and Human Dirofilariosis in Aveiro, Portugal: A One Health Perspective. Animals (Basel). 2025;15:952. https://doi.org/10.3390/ani15070952.
16. Johnson EE, Escobar LE, Zambrana-Torrelio C. An ecological framework for modeling the geography of disease transmission. Trends Ecol Evol. 2019;34:655–68. https://doi.org/10.1016/j.tree.2019.03.004.
17. Escobar LE. Ecological niche modeling: an introduction for veterinarians and epidemiologists. Front Vet Sci. 2020;7:519059.
18. Hill DE, Dubey JP, Baroch JA, Swafford SR, Fournet VF, Hawkins-Cooper D, et al. Surveillance of feral swine for *Trichinella* spp. and *Toxoplasma gondii* in the USA and host-related factors associated with infection. Vet Parasitol. 2014;205:653–65. https://doi.org/10.1016/j.vetpar.2014.07.026.
19. Chavy A, Ferreira Dales Nava A, Luz SLB, Ramírez JD, Herrera G, Vasconcelos Dos Santos T, et al. Ecological niche modelling for predicting the risk of cutaneous leishmaniasis in the Neotropical moist forest biome. PLoS Negl Trop Dis. 2019;13:e0007629. https://doi.org/10.1371/journal.pntd.0007629.
20. Meshgi B, Majidi-Rad M, Hanafi-Bojd AA, Fathi S. Ecological niche modeling for predicting the habitat suitability of fascioliasis based on maximum entropy model in southern Caspian Sea littoral, Iran. Acta Trop. 2019;198:105079. https://doi.org/10.1016/j.actatropica.2019.105079.
21. Meshgi B, Majidi-Rad M, Hanafi-Bojd AA, Kazemzadeh A. Predicting environmental suitability and geographical distribution of *Dicrocoelium dendriticum* at littoral of Caspian Sea: an ecological niche-based modeling. Prev Vet Med. 2019;170:104736. https://doi.org/10.1016/j.prevetmed.2019.104736.
22. Giannakopoulos A, Tsokana CN, Pervanidou D, Papadopoulos E, Papaspyropoulos K, Spyrou V, et al. Environmental parameters as risk factors for human and canine *Leishmania* infection in Thessaly, Central Greece. Parasitology. 2016;143:1179–86. https://doi.org/10.1017/S0031182016000378.
23. Signorini M, Cassini R, Drigo M, Frangipane di Regalbono A, Pietrobelli M, Montarsi F, Stensgaard AS. Ecological niche model of *Phlebotomus perniciosus*, the main vector of canine leishmaniasis in north-eastern Italy. Geospatial Health. 2014;9:193–201. https://doi.org/10.4081/gh.2014.16.
24. Bozorg-Omid F, Youssefi F, Hassanpour G, Rahimi Foroushani A, Rahimi M, Shirzadi MR, et al. Predicting the effect of temperature changes on *Phlebotomus papatasi* activity, as the main vector of zoonotic cutaneous leishmaniasis in Iran. Transbound Emerg Dis. 2025;2025:9518371. https://doi.org/10.1155/tbed/9518371.
25. Rodríguez-Escolar I, Hernández-Lambraño RE, Sánchez-Agudo JÁ, Collado M, Pérez-Pérez P, Morchón R. Current risk of dirofilariosis transmission in the Iberian Peninsula (Spain and Portugal) and the Balearic Islands (Spain) and its future projection under climate change scenarios. Animals. 2023;13:1764. https://doi.org/10.3390/ani13111764.
26. Rodríguez-Escolar I, Balmori-de la Puente A, Collado-Cuadrado M, Bravo-Barriga D, Delacour-Estrella S, Hernández-Lambraño RE, Sánchez Agudo JÁ, Morchón R. Analysis of the current risk of *Leishmania infantum* transmission for domestic dogs in Spain and Portugal and its future projection in climate change scenarios. Front Vet Sci. 2024;11:1399772. https://doi.org/10.3389/fvets.2024.1399772.
27. Balmori-de la Puente A, Rodríguez-Escolar I, Collado-Cuadrado M, Infante González-Mohino E, Vieira Lista MC, Hernández-Lambraño RE, Sánchez-Agudo JÁ, Morchón R. Transmission risk of vector-borne bacterial diseases (*Anaplasma* spp. and *Ehrlichia canis*) in Spain and Portugal. BMC Vet Res. 2024;20:526. https://doi.org/10.1186/s12917-024-04383-3.
28. Genchi C, Mortarino M, Rinaldi L, Cringoli G, Traldi G, Genchi M. Changing climate and changing vector-borne disease distribution: the example of *Dirofilaria* in Europe. Vet Parasitol. 2011;176:295–9. https://doi.org/10.1016/j.vetpar.2011.01.012.
29. Rinaldi L, Musella V, Biggeri A, Cringoli G. New insights into the application of geographical information systems and remote sensing in veterinary parasitology. Geospat Health. 2006;1:33–47. https://doi.org/10.4081/gh.2006.279.
30. Simón L, Afonin A, López-Díez LI, González-Miguel J, Morchón R, Carretón E, et al. Geo-environmental model for the prediction of potential transmission risk of *Dirofilaria* in an area with dry climate and extensive irrigated crops. The case of Spain. Vet Parasitol. 2014;200:257–64. https://doi.org/10.1016/j.vetpar.2013.12.027.
31. Medlock JM, Barrass I, Kerrod E, Taylor MA, Leach S. Analysis of climatic predictions for extrinsic incubation of *Dirofilaria* in the United kingdom. Vector Borne Zoonotic Dis. 2007;7:4–14. https://doi.org/10.1089/vbz.2006.0564.
32. Mortarino M, Musella V, Costa V, Genchi C, Cringoli G, Rinaldi L. Gis modeling for canine dirofilariosis risk assessment in central Italy. Geospat Health. 2008;2:253–61. https://doi.org/10.4081/gh.2008.248.
33. Rinaldi L, Genchi C, Musella V, Genchi M, Cringoli G. Geographical information systems as a tool in the control of heartworm infections in dogs and cats. Vet Parasitol. 2011;176:286–90. https://doi.org/10.1016/j.vetpar.2011.01.010.
34. Sassnau R, Czajka C, Kronefeld M, Werner D, Genchi C, Tannich E, et al. *Dirofilaria repens* and *Dirofilaria immitis* DNA findings in mosquitoes in Germany: temperature data allow autochthonous extrinsic development. Parasitol Res. 2014;113:3057–61. https://doi.org/10.1007/s00436-014-3970-1.
35. Kartashev V, Afonin A, González-Miguel J, Sepúlveda R, Simón L, Morchón R, et al. Regional warming and emerging vector-borne zoonotic dirofilariosis in the Russian Federation, Ukraine, and other post-Soviet states from 1981 to 2011 and projection by 2030. Biomed Res Int. 2014;2024:858936. https://doi.org/10.1155/2014/858936.
36. Ciucă L, Musella V, Miron LD, Maurelli MP, Cringoli G, Bosco A, et al. Geographic distribution of canine heartworm (*Dirofilaria immitis*) infection in stray dogs of eastern Romania. Geospatioal Health. 2016;11:499. https://doi.org/10.4081/gh.2016.499.
37. Farkas R, Mag V, Gyurkovszky M, Takács N, Vörös K, Solymosi N. The current situation of canine dirofilariosis in Hungary. Parasitol Res. 2020;119:129–35. https://doi.org/10.1007/s00436-019-06478-5.
38. Morchón R, Rodríguez-Escolar I, Lambraño REH, Agudo JÁS, Montoya-Alonso JA, Serafín-Pérez I, et al. Assessment heartworm disease in the Canary Islands (Spain): risk of transmission in a hyperendemic area by ecological niche modeling and its future projection. Animals. 2023;13:3251. https://doi.org/10.3390/ani13203251.
39. Rodríguez-Escolar I, Hernández-Lambraño RE, Sánchez-Agudo JÁ, Collado-Cuadrado M, Savić S, Žekić Stosic M, et al. Prediction and validation of potential transmission risk of *Dirofilaria* spp. infection in Serbia and its projection to 2080. Front Vet Sci. 2024;11:1352236. https://doi.org/10.3389/fvets.2024.1352236.
40. Rodríguez-Escolar I, Hernández-Lambraño RE, Sánchez-Agudo JÁ, Collado-Cuadrado M, Sioutas G, Papadopoulos E, et al. Ecological niche modeling analysis (*Cx. pipiens*), potential risk and projection of *Dirofilaria* spp. infection in Greece. Vet Parasitol. 2024;328:110172. https://doi.org/10.1016/j.vetpar.2024.110172.

41. Genchi M, Escolar IR, García RM, Semeraro M, Kramer LH, Colombo L, et al. *Dirofilaria immitis* in Italian cats and the risk of exposure by *Aedes albopictus*. Vector-Borne Zoonotic Dis. 2024;24:151–8. https://doi.org/10.1089/vbz.2023.0097.
42. Genchi C, Rinaldi L, Cascone C, Mortarino M, Cringoli G. Is heartworm disease really spreading in Europe? Vet Parasitol. 2005;133:137–48. https://doi.org/10.1016/j.vetpar.2005.04.009.
43. Genchi C, Rinaldi L, Mortarino M, Genchi M, Cringoli G. Climate and *Dirofilaria* infection in Europe. Vet Parasitol. 2009;163:286–92. https://doi.org/10.1016/j.vetpar.2009.03.026.
44. Berentsen WH, Poulsen TM, Windley BF, East WG. Europe. In: Encyclopedia Britannica. 2025. https://www.britannica.com/place/Europe. Accessed 29 May 2025.
45. Climate Shifts. InWorldmaps of Köppen-Geiger Climate Classification. 2019. http://koeppen-geiger.vuwien.ac.at/shifts.html. Accessed 31 July 2025.
46. Antonescu B, Mărmureanu L, Vasilescu J, Marin C, Andrei S, Boldeanu M, et al. A 41-year bioclimatology of thermal stress in Europe. Int J Climatol. 2021;41:3934–52. https://doi.org/10.1002/joc.7051.
47. GBIF.org. GBIF Occurrence Download. 2025. https://www.gbif.org/. Accessed 29 November 2024.
48. ECDPC. European Centre for Disease Prevention and Control. 2024. Available at https://www.ecdc.europa.eu/en/about-us/partnerships-and-networks/disease-and-laboratory-networks/vector-net. Accessed 14 February 2025.
49. Gangoso L, Aragonés D, Martínez-de la Puente J, Lucientes J, Delacour-Estrella S, Estrada Peña R, et al. Determinants of the current and future distribution of the West Nile virus mosquito vector *Culex pipiens* in Spain. Environ Res. 2020;188:109837. https://doi.org/10.1016/j.envres.2020.109837.
50. Ferreira CA, de Pinho MV, Novo MT, Calado MM, Gonçalves LA, Belo SM, et al. First molecular identification of mosquito vectors of *Dirofilaria immitis* in continental Portugal. Paras Vect. 2015;8:139. https://doi.org/10.1186/s13071-015-0760-2.
51. Spanoudis CG, Pappas CS, Savopoulou-Soultani M, Andreadis SS. Composition, seasonal abundance, and public health importance of mosquito species in the regional unit of Thessaloniki, Northern Greece. Parasitol Res. 2021;120:3083–90. https://doi.org/10.1007/s00436-021-07264-y.
52. Fotakis EA, Mavridis K, Kampouraki A, Balaska S, Tanti F, Vlachos G, et al. Mosquito population structure, pathogen surveillance and insecticide resistance monitoring in urban regions of Crete, Greece. PLoS Negl Trop Dis. 2022;16:e0010186. https://doi.org/10.1371/journal.pntd.0010186.
53. Patsoula E, Beleri S, Tegos N, Mkrtsian R, Vakali A, Pervanidou D. Entomological data and detection of West Nile virus in mosquitoes in Greece (2014–2016), before disease re-emergence in 2017. Vector Borne Zoonotic Dis. 2020;20:60–70. https://doi.org/10.1089/vbz.2018.2422.
54. Kurucz K, Kepner A, Krtinic B, Zana B, Földes F, Bányai K, et al. First molecular identification of *Dirofilaria* spp. (Onchocercidae) in mosquitoes from Serbia. Parasitol Res. 2016;115:3257–60. https://doi.org/10.1007/s00436-016-5126-y.
55. Kemenesi G, Buzás D, Zana B, Kurucz K, Krtinic B, Kepner A, et al. First genetic characterization of Usutu virus from *Culex pipiens* mosquitoes Serbia, 2014. Infect Genet Evol. 2018;63:58–61. https://doi.org/10.1016/j.meegid.2018.05.012.
56. Južnič-Zonta Ž, Sanpera-Calbet I, Eritja R, Palmer JRB, Escobar A, Garriga J, et al. Mosquito alert: leveraging citizen science to create a GBIF mosquito occurrence dataset. GigaByte. 2022;2022:gigabyte54. https://doi.org/10.46471/gigabyte.54.
57. Morchón R, Carretón E, González-Miguel J, Mellado-Hernández I. Heartworm disease (*Dirofilaria immitis*) and their vectors in Europe-new distribution trends. Front Physiol. 2012;3:196. https://doi.org/10.3389/fphys.2012.00196.
58. WorldClim. Bioclimatic variables. 2024. https://www.worldclim.org/data/bioclim.html. Accessed 29 November 2024.
59. R Core Team. In: R: a language and environment for statistical computing. R Foundation for Statistical Computing. https://www.r-project.org/. Accessed 29 November 2024.
60. Cobos ME, Peterson AT, Barve N, Osorio-Olvera L. kuenm: an R package for detailed development of ecological niche models using Maxent. PeerJ. 2019;7:e6281. https://doi.org/10.7717/peerj.6281.
61. Socioeconomic Data and Applications Center (SEDAC). 2024. https://sedac.ciesin.columbia.edu. Accessed 29 November 2024.
62. Corine Land Cover. 2018. https://datos.gob.es/es/catalogo/e00125901-spaignclc2018. Accessed 29 November 2024.
63. EarthEnv. Global, remote-sensing supported environmental layers for assessing status and trends in biodiversity, ecosystems, and. 2024. https://www.earthenv.org/. Accessed 29 November 2024.
64. Phillips SJ, Anderson RP, Schapire RE. Maximum entropy modeling of species geographic distributions. Ecol Modell. 2006;190:231–59. https://doi.org/10.1016/j.ecolmodel.2005.03.026.
65. CHELSA. Climatologies at high resolution for the Earth's land surface areas. 2024. https://chelsa-climate.org/. Accessed 29 November 2024.
66. myVBDmap. CEVA Santé Animale. 2025. https://www.myvbdmap.com/es. Accessed 24 June 2025.
67. Kosić SL, Simin S, Lalosevic S, Lalošević V, Lalošević D, Kuruca L, Nikolć S, Nerac D. Updating the prevalence of canine dirofilariosis in pet dogs in Novi Sad, Vojvodina, Serbia. Contemporary Agriculture. 2014;63:487–493. UDC: 636.09:569.74.
68. Savic S, Vidic B, Grgic Z, Petrovic T, Potkonjak A, Cupina A, Vaselek S. Dirofilariosis and leishmaniasis in the northern region of Serbia. In: An overview of tropical diseases. InTech. 2015. https://doi.org/10.5772/61761. Accessed 2 February 2025.
69. Alho AM, Meireles J, Schnyder M, Cardoso L, Belo S, Deplazes P, et al. *Dirofilaria immitis* and *Angiostrongylus vasorum*: the current situation of two major canine heartworms in Portugal. Vet Parasitol. 2018;252:120–6. https://doi.org/10.1016/j.vetpar.2018.01.008.
70. Angelou A, Gelasakis AI, Verde N, Pantchev N, Schaper R, Chandrashekar R, et al. Prevalence and risk factors for selected canine vector-borne diseases in Greece. Parasit Vectors. 2019;12:283. https://doi.org/10.1186/s13071-019-3543-3.
71. Laidoudi Y, Ringot D, Watier-Grillot S, Davoust B, Mediannikov O. A cardiac and subcutaneous canine dirofilariosis outbreak in a kennel in central France. Parasite. 2019;26:72. https://doi.org/10.1051/parasite/2019073.
72. Kulmer LM, Unterköfler MS, Fuehrer HP, Janovska V, Pagac M, Svoboda M, et al. First autochthonous infection of a cat with *Dirofilaria immitis* in Austria. Pathogens. 2021;10:1104. https://doi.org/10.3390/pathogens10091104.
73. Tasić-Otašević S, Savić S, Jurhar-Pavlova M, Stefanovska J, Stalević M, Ignjatović A, et al. Molecular survey of *Dirofilaria* and *Leishmania* species in dogs from Central Balkan. Animals. 2022;12:911. https://doi.org/10.3390/ani12070911.
74. Montoya-Alonso JA, Morchón R, García-Rodríguez SN, Falcón-Cordón Y, Costa-Rodríguez N, Matos JI, et al. Expansion of canine heartworm in Spain. Animals Basel. 2022;12:1268. https://doi.org/10.3390/ani12101268.
75. Kuhlbrodt T, Jones CG, Sellar A, Storkey D, Blockley E, Stringer M, et al. The low-resolution version of HadGEM3 GC3.1: development and evaluation for global climate. J Adv Model Earth Syst. 2018;10:2865–88. https://doi.org/10.1029/2018MS001370.
76. Andrews MB, Ridley JK, Wood RA, Andrews T, Blockley EW, Booth B, et al. Historical simulations with HadGEM3-GC3. 1 for CMIP6. J Adv Model Earth Syst. 2020;12:e2019MS001995. https://doi.org/10.1029/2019MS001995.
77. Zelinka MD, Myers TA, McCoy DT, Po-Chedley S, Caldwell PM, Ceppi P, Klein SA, Taylor KE. Causes of higher climate sensitivity in CMIP6 models. Geophys Res Lett. 2020;47:e2019GL085782. https://doi.org/10.1029/2019GL085782.
78. Palmer TE, McSweeney CF, Booth BB, Priestley MD, Davini P, Brunner L, et al. Performance-based sub-selection of CMIP6 models for impact assessments in Europe. Earth Syst Dyn. 2023;14:457–83. https://doi.org/10.5194/esd-14-457-2023.
79. Thuiller W, Lafourcade W, Lafourcade B, Engler R, Araújo MB. BIOMOD–A platform for ensemble forecasting of species distributions. Ecography. 2009;32:369–73. https://doi.org/10.1111/j.1600-0587.2008.05742.x.
80. Montoya-Alonso JA, Carretón E, Simón L, González-Miguel J, García-Guasch L, Morchón R, et al. Prevalence of *Dirofilaria immitis* in dogs from Barcelona: validation of a geospatial prediction model. Vet Parasitol. 2015;212:456–9. https://doi.org/10.1016/j.vetpar.2015.06.025.
81. Mordecai EA, Caldwell JM, Grossman MK, Lippi CA, Johnson LR, Neira M, et al. Thermal biology of mosquito-borne disease. Ecol Lett. 2019;22:1690–708. https://doi.org/10.1111/ele.13335.
82. Ligsay A, Telle O, Paul R. Challenges to mitigating the urban health burden of mosquito-borne diseases in the face of climate change. Int

J Environ Res Public Health. 2021;18:5035. https://doi.org/10.3390/ijerph18095035.
83. de Mendonça SF, Rocha MN, Ferreira FV, Leite THJF, Amadou SCG, Sucupira PHF, et al. Evaluation of *Aedes aegypti*, *Aedes albopictus*, and *Culex quinquefasciatus* mosquitoes competence to Oropouche virus infection. Viruses. 2021;13:755. https://doi.org/10.3390/v13050755.
84. Hanafi-Bojd AA, Vatandoost H, Yaghoobi-Ershadi MR. Climate change and the risk of malaria transmission in Iran. J Med Entomol. 2020;57:50–64. https://doi.org/10.1093/jme/tjz131.
85. Githeko AK, Lindsay SW, Confalonieri UE, Patz JA. Climate change and vector-borne diseases: a regional analysis. Bull World Health Organ. 2000;78:1136–47.
86. Semenza JC, Menne B. Climate change and infectious diseases in Europe. Lancet Infect Dis. 2009;9:365–75. https://doi.org/10.1016/S1473-3099(09)70104-5.
87. Hongoh V, Berrang-Ford L, Scott ME, Lindsay LR. Expanding geographical distribution of the mosquito, *Culex pipiens*, in Canada under climate change. Appl Geogr. 2012;33:53–62. https://doi.org/10.1016/j.apgeog.2011.05.015.
88. Charrahy Z, Yaghoobi-Ershadi MR, Shirzadi MR, Akhavan AA, Rassi Y, Hosseini SZ, et al. Climate change and its effect on the vulnerability to zoonotic cutaneous leishmaniasis in Iran. Transbound Emerg Dis. 2022;69:1506–20. https://doi.org/10.1111/tbed.14115.
89. Koch LK, Kochmann J, Klimpel S, Cunze S. Modeling the climatic suitability of leishmaniasis vector species in Europe. Sci Rep. 2017;7:13325. https://doi.org/10.1038/s41598-017-13822-1.
90. Sofizadeh A, Rassi Y, Vatandoost H, Hanafi-Bojd AA, Mollalo A, Rafizadeh S, et al. Predicting the distribution of *Phlebotomus papatasi* (Diptera: Psychodidae), the primary vector of zoonotic cutaneous leishmaniasis, in Golestan Province of Iran using ecological niche modeling: comparison of MaxEnt and GARP models. J Med Entomol. 2017;54:312–20. https://doi.org/10.1093/jme/tjw178.
91. Chalghaf B, Chemkhi J, Mayala B, Harrabi M, Benie GB, Michael E, et al. Ecological niche modeling predicting the potential distribution of *Leishmania* vectors in the Mediterranean basin: impact of climate change. Parasit Vectors. 2018;11:461. https://doi.org/10.1186/s13071-018-3019-x.
92. Omar K, Thabet HS, TagEldin RA, Asadu CC, Chukwuekezie OC, Ochu JC, et al. Ecological niche modeling for predicting the potential geographical distribution of *Aedes* species (Diptera: Culicidae): a case study of Enugu State, Nigeria. Parasite Epidemiol Control. 2021;15:e00225. https://doi.org/10.1016/j.parepi.2021.e00225.
93. Di X, Li S, Ma B, Di X, Li Y, An B, et al. How climate, landscape, and economic changes increase the exposure of *Echinococcus* spp. BMC Public Health. 2022;22:2315.
94. Kuyucu AC, Hekimoglu O. Predicting the distribution of *Ixodes ricinus* in Europe: integrating microclimatic factors into ecological niche models. Parasitology. 2024;151:1012–23.
95. Tian D, Cui XM, Ye RZ, Li YY, Wang N, Gao WY, et al. Distribution and diversity of ticks determined by environmental factors in Ningxia, China. One Health. 2024;19:100897. https://doi.org/10.1016/j.onehlt.2024.100897.

Publisher's Note